Evaluation of Thermally Sprayed Coatings Under Reciprocating Lubricated Wear Conditions

S. Usmani and K.N. Tandon

To find an alternate coating to hard electroplated chrome in internal combustion engines, wear tests and metallurgical characterization have been performed on plasma-sprayed chromium oxide, metal-arc-sprayed martensitic stainless steel, and electroplated chromium coatings applied to steel base material. A wear test rig was fabricated that simulated the reciprocating sliding wear under lubrication encountered in internal combustion engines. The chromium oxide coating was found to perform equally well compared to the hard chrome coating that is conventionally used.

1. Introduction

THE past decade has seen an increased use of thermal spraying for applying wear-resistant coatings in many unique applications. Specifically, there appears to be an increased interest in plasma- and arc-sprayed coatings.[1-4] These processes offer a rapid and efficient method of depositing a variety of materials onto metallic substrates. In this article, two coatings deposited by such processes are evaluated as alternative materials to electrochemically deposited chromium for a wear-resistant surface in diesel engine liners.

The process of electrodeposition of chromium is a very slow process (0.001 in./hr, or 0.03 mm/hr) that entails the disposition of hazardous chemicals from the process into the environment. Moreover, electrodeposited chromium coatings experience stress cracking,[5,6] expensive post-plating treatment,[6] and peeling under severe operating conditions,[7] thus limiting the application of this kind of wear-resistant surface. Thermal spraying on the other hand is a faster, easy to apply, and economical process. However, to achieve optimum results, the performance of thermally sprayed coatings needs to be evaluated for each individual application.[8-13] Although information is available on wear testing,[8-15] bond strength testing,[4,8,10] microscopy, and structure/property relationships[5,10-16] of the various thermally sprayed coatings, it nevertheless becomes necessary to qualitatively and quantitatively evaluate the coatings for specific wear applications.

In the present work, the lubricated, reciprocating, sliding wear performance of martensitic stainless steel (AISI type 420, 0.3% C, 13.5% Cr steel, coded "AS") and plasma-sprayed Cr_2O_3 (coded as "PC") was compared with that of electrochemically deposited chromium (coded as "EC"). The sprayed coatings were selected for evaluation because stainless steel has been claimed to be an all-purpose wear-resistant material,[5] and Cr_2O_3-based coatings deposited using other processes have performed well in some wear tests.[8,10] However, the lubricated, reciprocating, sliding wear performance of the selected sprayed coatings has not yet been evaluated. In the present work, the wear performance of the selected coatings are related to wear mechanism studies previously reported in the literature.[10-15] In addition to wear tests, bond strength testing and microstructural characterization of the coatings were also performed.

Key Words: electroplating comparison, internal combustion engines, porosity, reciprocating sliding wear, roughness, wear testing

S. Usmani, graduate student, and **K.N. Tandon**, Associate Professor, Department of Mechanical and Industrial Engineering, MRC-AIM Initiative, University of Manitoba, Winnipeg, Manitoba, Canada.

2. Experimental Procedure

The coated specimens were prepared by using a TAFA metal arc gun and TAFA 60TB wire for the AS coatings, a Metco plasma gun and Cr_2O_3 powder (METCO 106FP-NS) for the PC coatings, and an electrochemical hard chrome process for the EC coatings. Manufacturers' specifications for producing the coatings were followed during the application. Wear test specimens were ground and polished to achieve flat and similar surfaces (0.10 to 0.36 μm, R_a). The characterization of the test specimens was carried out by means of hardness measurements, surface profilometry, and optical and scanning electron microscopy (SEM). Energy-dispersive spectroscopy (EDS) was performed where necessary.

Hardness measurements were conducted on specimen cross sections using a Leitz microhardness tester at a load of 300 g. Surface profilometry was performed on the polished surfaces before wear testing. After wear testing, the trace of the wear track was recorded so that the wear volume could be calculated. The surface profile measuring system used was the Surtronic 3P. Microstructural analysis of the coating was performed using a Nikon inverted optical microscope and a JEOL JXA-840 SEM. The Cr_2O_3-coated specimens were sputtered with gold prior to SEM observations.

Adhesive/cohesive strength tests were conducted to determine the bond strength of the AS and PC coatings sprayed on ductile cast iron coupons (25.4 mm in diameter and 50.8 mm long) as per the ASTM C633-79 test method, "Adhesion or Cohesive Strength of Flame Sprayed Coatings." The surfaces of the loading and substrate fixtures were glued together using an epoxy (CIBA-GEIGY FM 1000) adhesive cured at 170 ± 5 °C for 60 min. The surfaces were compressed by a support device

that maintained axial alignments. This entire assembly was kept in the oven so that the adhesive could achieve the maximum cured strength. The pull-off test was subsequently performed at a rate of 0.001 mm/s in an Instron model 1137 tensile testing machine, modified according to the testing requirements of the above-stated test method. The load at failure and the type of failure were recorded for each test.

The wear test coupons were prepared by applying the coatings on one 50- by 25-mm face of 50- by 25- by 6-mm pieces of mild steel. The tests were conducted under constant-load conditions on a custom-built wear test rig (Fig. 1). The sliding material on all the test surfaces was a martensitic nodular cast iron piston ring used in locomotive diesel engines. Other parameters of the wear tests are given in Table 1.

Table 1 Wear Test Parameters

Cycles per minute	415
Wear track length, mm	30
Sliding distance per cycle, mm	2 × 30
Contact load, N	98,196,392
Number of cycles slid	200,000
Lubricant	10W30 oil at 24 °C
Lubrication rate	1 drop every 240 sec (one drop = 0.02 ml)
Surrounding atmosphere	Laboratory air
Humidity, (%)	38 to 40
Specimen heated to	80 °C
Angle to ground	10 °

The operation of the test rig shown in Fig. 1 can be outlined as follows. The specimen (1) with the coating on its top surface was held in place in a specimen holder (2). The piston ring (3) was held in a piston ring holder (4), which was attached to a slider (5), whose reciprocating motion on two hardened shafts (6) was facilitated by a drive mechanism (7) through a connecting rod (8). The contact between the two surfaces was produced by the application of load (9), which lifted the specimen holder with a parallel arm-linkage mechanism (10). The lubricant drop (11) rate was controlled using a needle valve (12) connected to a lubricant reservoir. The temperature of the specimen could also be controlled by a set of heaters embedded into the sample holder plate (13). The main setup of the rig was adjusted at an angle to the ground by using adjustable support bars (14) fixed on the frame (15). Thus, the oil flowed down where it was collected in a reservoir (16). The concept of this rig is similar to that of some other test rigs.[6,11,17] In the present work, the specimen was oriented at an angle (10°) to the ground to ensure that all the lubricant reached the wear surface, but did not accumulate at the sliding surface.

The amount of wear was determined using the surface profile measuring system described earlier. The effect of initial roughness on these measurements was insignificant. It was used to plot the cross-sectional area of the wear track formed on the test

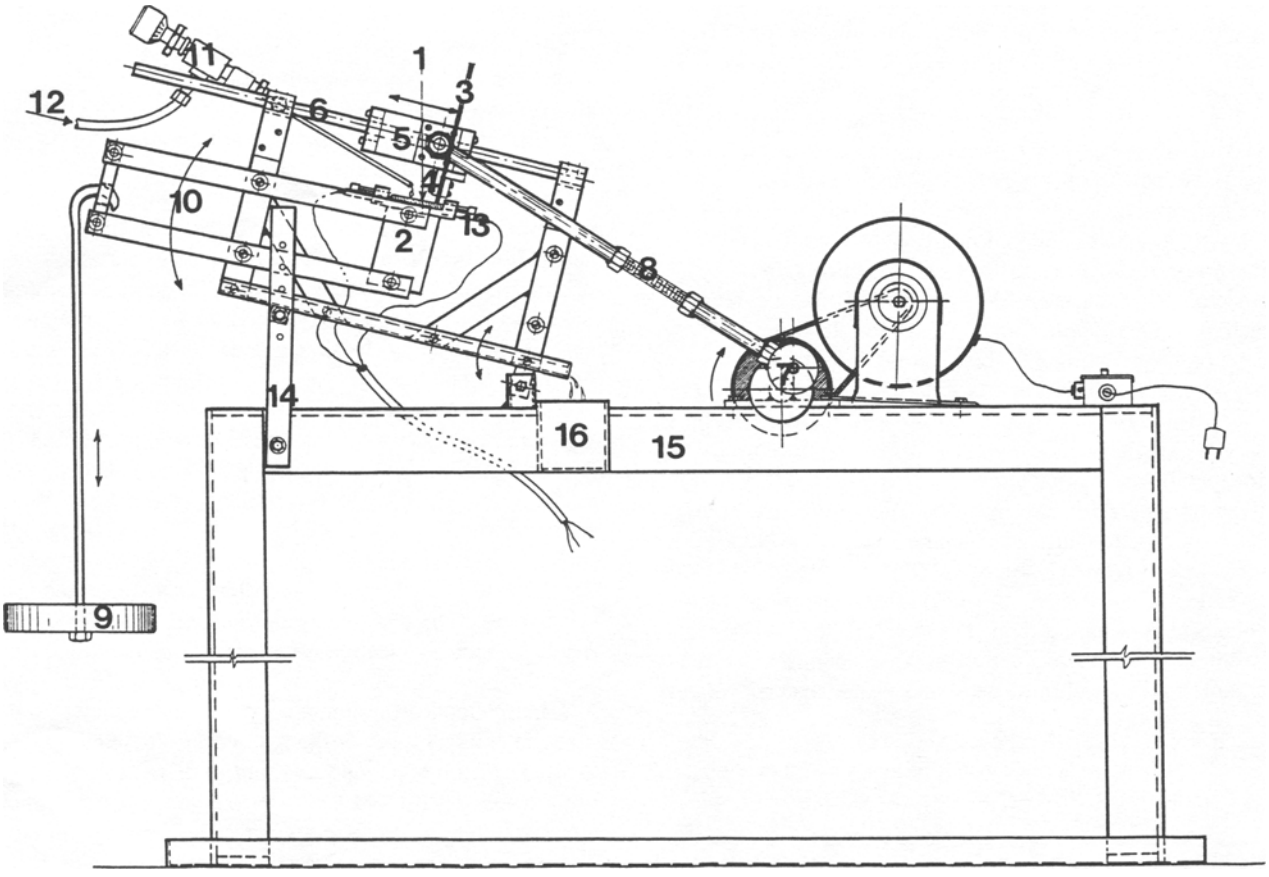

Figure 1 Wear test rig. See text for component identification.

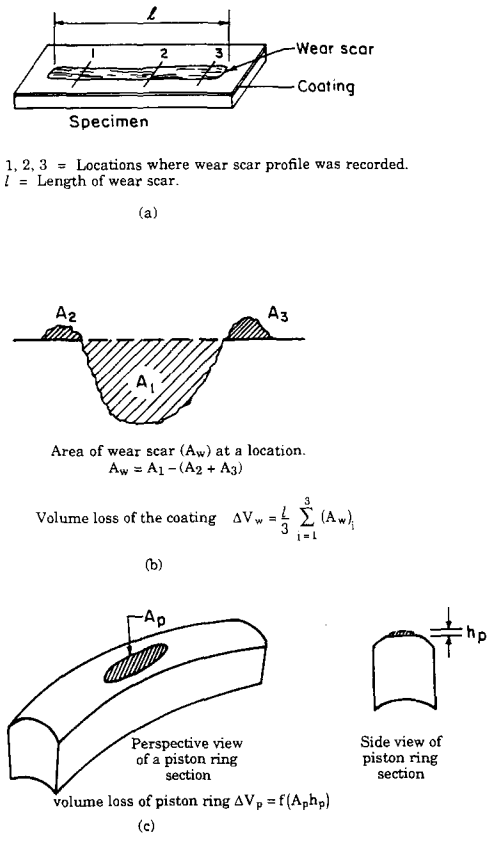

Figure 2 Calculation of cross-sectional area and volume loss of the coating wear scar (**a**) and (**b**) and piston ring wear (**c**).

surface (Fig. 2a and b). The mean of the area from three profiles along the scar was then used to calculate the volume loss of the material by taking the product of this area and the length of the groove, which was the length of one forward or backward movement of the piston ring. This technique of wear quantification is very similar to that used by other researchers.[18] The volume loss of the piston ring was determined by taking an impression of the worn surface area on the piston ring using a semitransparent tape, which could be closely approximated to a shape such as that of an ellipse (Fig. 2c). The loss in the thickness of the piston ring for a wear scar (Fig. 2c) was used to calculate the appropriate volume loss for a wear spot. The loss in volume was then converted to mass loss using the appropriate material densities.

3. Results and Discussion

The microstructural cross-sections of the AS, PC, and EC coatings are shown in Fig. 3(a), (b), and (c), respectively. Figure 3(d) is a SEM secondary electron image of the piston ring substrate material. These figures indicate the formation of a splat-like microstructure, typical of thermally sprayed coatings (AS and PC).[2] The electrochemically deposited chromium (hard chrome), on the other hand, has a much more uniform and dense structure (Fig. 3c). Some stress cracking vertical to the substrate

Table 2 Cross-Sectional Hardness and Surface Roughness Values

Coating	Material	Hardness DPH (300 g)	Roughness (R_a), μm
CI	Piston ring, cast iron	427	1.80
AS	Arc-sprayed martensitic stainless steel	262	0.36
PC	Plasma-sprayed Cr_2O_3	533	0.33
EC	Electrochemically deposited (hard chrome) chromium	927	0.10

Table 3 Adhesion Test Results (ASTM C633-79)

Specimen	Average roughness (R_a), μm	Stress at failure, MPa	Mode of failure
Plasma-sprayed Cr_2O_3 on cast iron (PC)			
1	4.3	6.92	Cohesive
2	4.5	1.79	Cohesive/adhesive(a)
3	4.0	6.82	Cohesive
4	4.5	4.39	Cohesive
5	4.6	3.55	Cohesive
Average	4.4	4.69	
Arc-sprayed martensitic stainless steel (AS)			
1	15.0	5.72	Adhesive
2	14.5	16.08	Cohesive
3	16.0	15.45	Cohesive
4	16.2	17.50	Cohesive
5	14.7	6.59	Adhesive
Average	15.3	12.26	

(**a**) Failure occurred both at the epoxy and inside the coating.

surface, typical of hard chrome,[5] was noted in the EC coating. The micrograph of the piston ring cross section (Fig. 3d) reveals that it has a martensitic nodular cast iron microstructure.

The hardness and surface roughness values for the three coatings and the cast iron (CI) piston ring are given in Table 2. Note that the hard chrome had the smoothest surface, which could be attributed to the dense nature of the electroplated chromium. On the other hand, thermally sprayed AS and PC coatings had a characteristically lamellar structure, that contributed to the surface roughness. The chromium coating was the hardest of the three coatings, followed by plasma-sprayed Cr_2O_3, and then arc-sprayed martensitic stainless steel.

Bond strength test data are given in Table 3, which indicates that the failure in both thermally sprayed coatings was cohesive. The strength at cohesive failure for the steel (AS) was about half that of the values reported by another group of investigators[4] for a similar coating. The failure type reported in both the investigations was cohesive. The discrepancy between the two bond strength results could be attributed to a possible variation in coating process parameters between the two investigations. Concerning the Cr_2O_3 (PC) coating, a similar work[10] reported adhesive failure at 2.84 MPa on the enamel substrate interface in a multilayered Cr_2O_3 coating. The cohesive strength of Cr_2O_3 under tension can thus be qualitatively assessed to be greater than 2.84 MPa. In the present work, a noteworthy reproducibil-

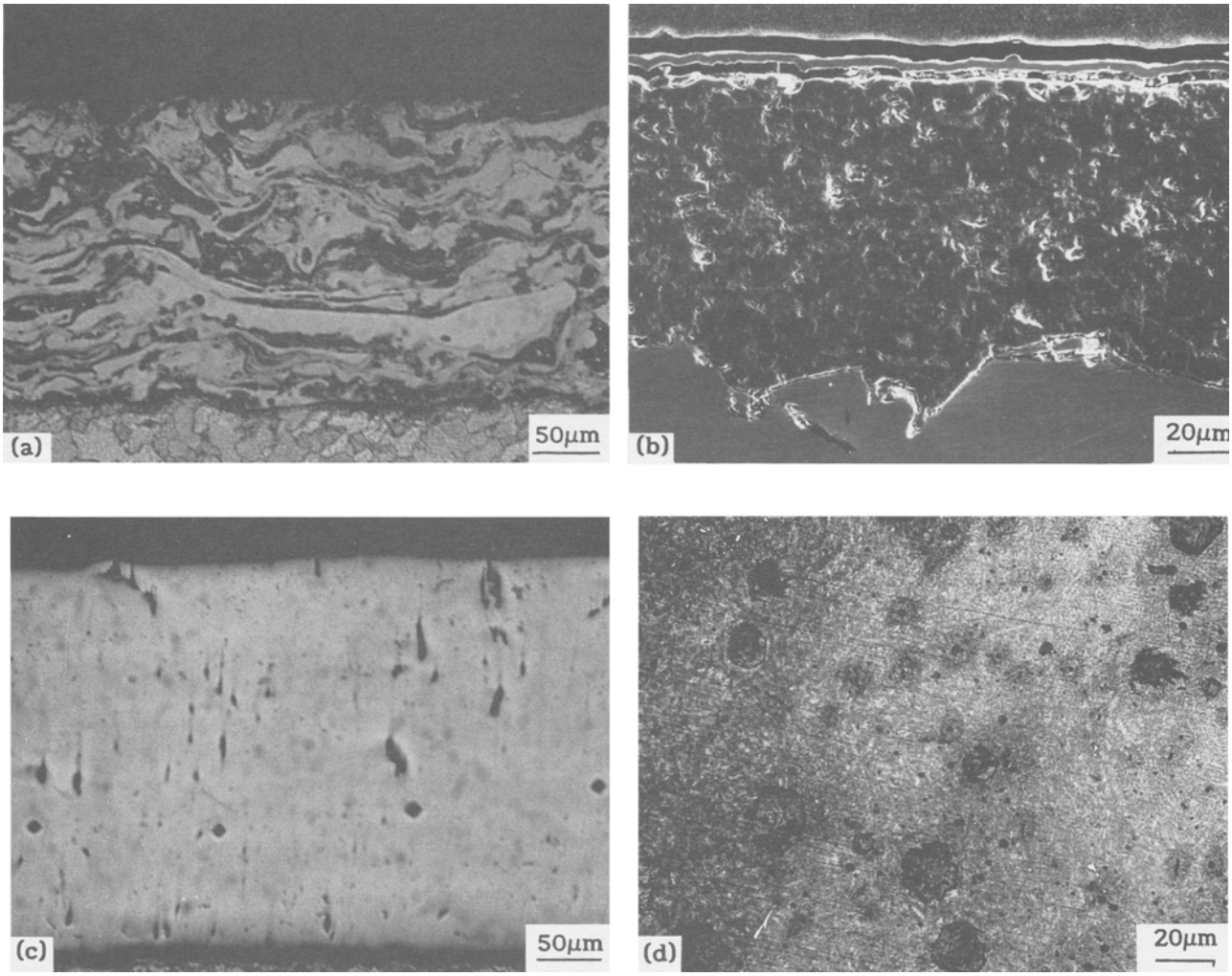

Figure 3 Micrographs of **(a)** arc-sprayed stainless steel coating (AS) (optical), **(b)** Plasma-sprayed Cr_2O_3 coating (PC) (SEM), **(c)** electroplated chromium coating (EC) (optical), and **(d)** cast-iron piston ring material (CI) (optical).

ity of the results and comparison with other results[4,10] provides confidence in the bond strength measurements. Moreover, it can be safely concluded from these results that the adhesion of the two coatings to the cast iron base is stronger than their respective cohesive strength values.

Wear tests were performed on the three coatings under the same lubrication conditions and the same piston ring (CI) for 200,000 cycles. The applied load was varied from 98 to 392 N. For each loading condition, loss in the mass of the coating and cast iron was determined using the techniques described earlier.

The mass loss of the coating material as a function of applied load for the three coatings is plotted in Fig. 4(a). For each case, the loss in the mass of cast iron is plotted in Fig. 4(b). The sum of the loss in mass of the coating and the corresponding cast iron mass loss is plotted in Fig. 4(c). Under severe conditions, it is the combined performance of both the mating surfaces that provides a true measure of wear.

Figure 4 indicates that the mass loss of the AS coating is higher than that of the other two coatings at all the load levels. In the case of mass loss of the piston ring sliding against an arc-sprayed coating, the value at the 392-N load level does not increase as dramatically above the 196-N load level as it does during sliding against the other two surfaces, which also are considerably harder than the AS coating. From these figures, it can be determined that the PC and EC coatings performed equally well, and both performed better than the AS coating.

The scanning electron micrographs of the wear surfaces of the coatings after 200,000 cycles of wear testing at the 392-N load are given in Fig. 5. The wear surface of the AS coating (Fig. 5a) was observed to have abrasive grooves (A), plastic flow (region near B), and wear debris compaction (C). Energy-dispersive spectroscopy revealed the presence of cast iron in this debris. The amount or fraction of cast iron could not be ascertained. However, the fraction of abrasive groove area to

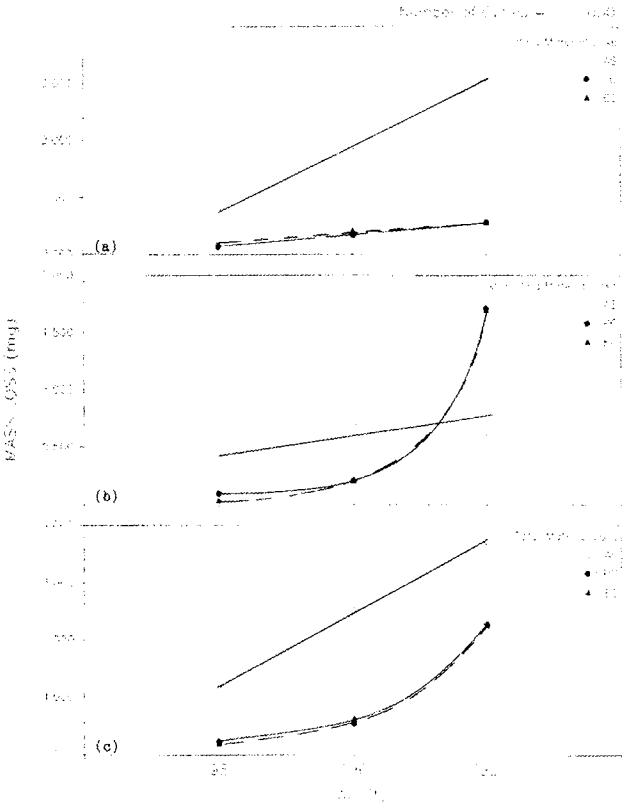

Figure 4 Mass loss of material during wear test of 200,000 cycles. **(a)** Coating material loss. **(b)** Piston ring material loss. **(c)** Total material loss.

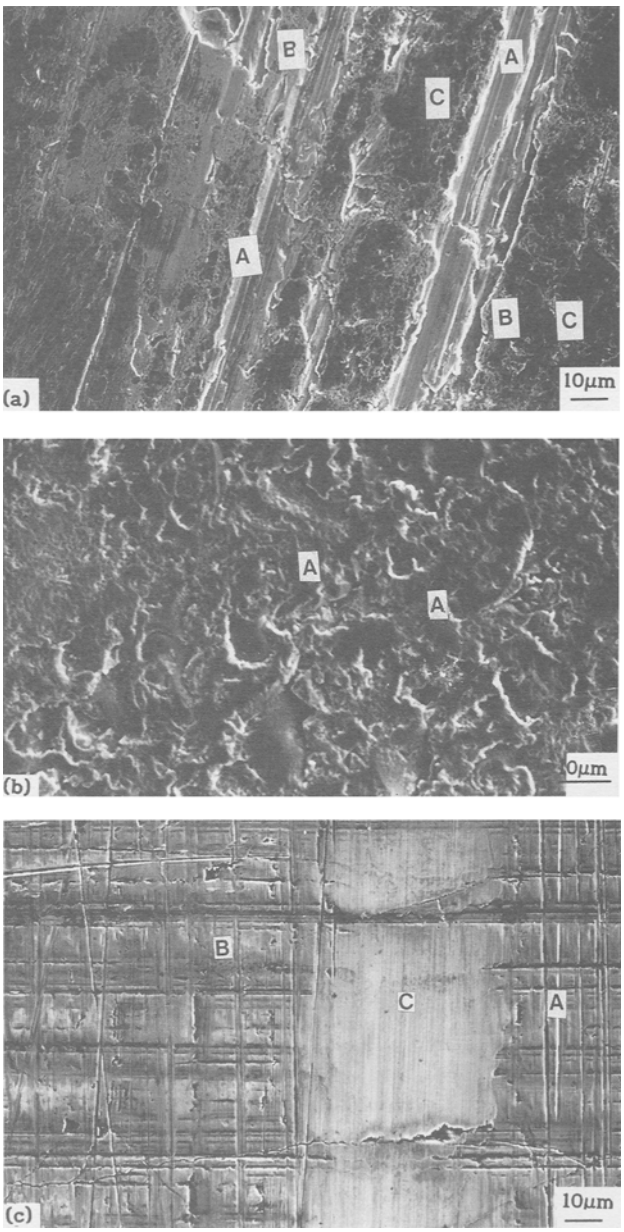

Figure 5 Scanning electron images of wear surface of **(a)** arc-sprayed stainless steel, **(b)** plasma-sprayed Cr_2O_3, and **(c)** electroplated after 200,000 cycles of lubricated, reciprocating sliding wear under 392-N load.

wear scar area was qualitatively estimated to be quite small. In the case of the PC coating (Fig. 5b), the wear was mainly due to mild abrasion or polishing (A). Evidence of any deep scratching or material transfer was not found. The polishing effect was also observed for the EC coating. Figure 5(c) shows the unworn portion (A), the polished portion (B), and a smooth groove (C) of the EC coating. The regular scratches are from the emery paper, in an attempt to roughen up the surface.

Typical wear surface profiles obtained from the profilometer are given in Fig. 6. The profiles of the worn thermally sprayed coatings (a and b) contain many sharp dips, indicating either particle pull-out or surface porosity of the coatings. The hard chrome, on the other hand, was comparatively smoother in the worn groove. These pore-like features in the thermally sprayed coatings are capable of retaining lubricant and wear debris.

The effect of the presence of a lubricant film in preventing severe wear has been discussed in the literature.[11,18-20] It is believed that the same beneficial effects are applicable in the present study. The surface porosity in the AS and PC coatings provides a natural reservoir for lubricant and wear debris, which further reduces severe wear. Moreover, the inclination of the specimen surface (10°) helps remove some wear debris with the flow of the lubricant.

A comparison of the lubricated sliding wear of the AS coating with that of carbon steel[18] reveals some similarities in the flow wear pattern of the two cases. In both cases, thin layers are extruded in the side direction by plastic flow of surface layers at the local spots of contact between the mating surfaces. However, no overlap of extruded layers from opposite layers was observed in the present case. Hence, the formation of loose wear debris due to the overlap of these layers, as observed in the case of carbon steel,[18] can be ruled out here.

The major portion of wear debris in the case of the AS coating is thought to have been generated by the fracture of surface asperities, as evidenced by micropitting in the surface profile of the wear scar (Fig. 6a). Due to the high contact stresses, the wear debris could be deformed and compacted into the surface cavi-

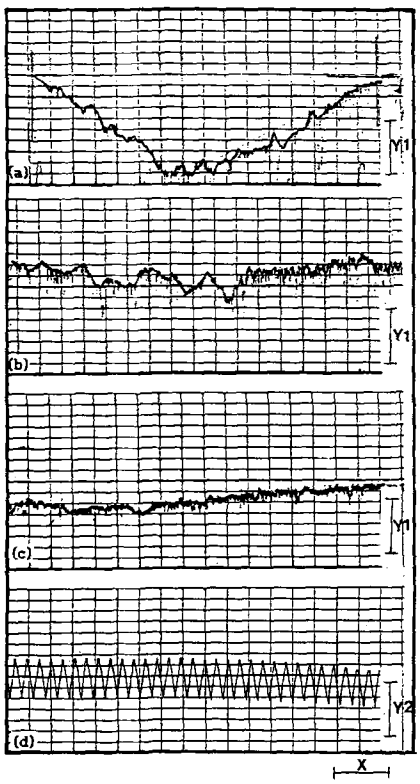

Figure 6 Typical surface profiles of the wear scar after wear tests of 200,000 cycles at 392-N load. **(a)** AS. **(b)** PC. **(c)** EC. **(d)** Calibration block.

ties. The effect of any local heating on subsequent melting and deforming of wear surface asperities or the wear debris could not be ascertained. Because no adhesive wear or severe abrasive wear was observed, the role of lubricant in preventing high wear rates and severe wear mechanisms, as reported elsewhere,[11,20] was confirmed. The limited number of abrasive grooves are thought to have been caused when a surface particle (such as a spalled asperity or a microchip) ploughed a furrow through the surface. The compacted wear debris is thought to have contributed to the smoothing of the wear scar (Fig. 6a).

In the case of the PC coating, mild polishing was noticed. High magnifications were required to resolve the details of the polishing wear processes. As shown in Fig. 5(b), the only apparent wear is due to the repeated polishing action of the piston ring, and large-scale abrasion is absent, signifying the absence of large or hard wear debris from the wear surface. The softer debris from abrasive wear of the piston ring contributed to surface polishing. It subsequently collected in the surface valleys and was also carried away from the wear zone by the flow of lubricant. Surface porosity and roughness in thermally sprayed coatings, therefore, contributed beneficially in reducing wear due to its ability to improve lubricant retention and also provide micrometer-sized reservoirs for collecting the wear debris.

The wear of the EC coating exhibits a combination of polishing and mild abrasion mechanisms (Fig. 5c). The surface of the specimen exhibits some polishing effects (B). The smooth groove (C) has formed due to the grinding action of a spalled asperity trapped between the mating surfaces under the high stress. The piston ring wear arose from abrasive action of hard surface asperities and any loosened surface particles trapped between the mating surfaces. Whatever debris that was generated either contributed to the polishing action (mild abrasion), or was collected in the surface micropits, or was carried away with the lubricant flow, as in the case of the PC coating.

4. Conclusions

A wear test arrangement for simulating lubricated, reciprocating, sliding wear was fabricated and successfully tested. The performance of plasma-sprayed Cr_2O_3 and hard chrome was found to be comparable under such wear test conditions. Surface polishing (mild abrasion) of the coating and abrasive wear of the piston ring were the major contributors to the wear in these two coatings.

The wear of arc-sprayed martensitic stainless steel was found to be more than that of the other two coatings because of its greater ductility. The major modes of wear for the steel were plastic deformation and ploughing (abrasive action). The wear debris that became compacted in the surface cavities contributed to a smoothing of the surface. The surface in thermally sprayed coatings was found to act as a reservoir for lubricant and wear debris, which alleviated wear of the coating.

Acknowledgments

Financial support to this project by the Transportation Development Centre (TDC), Transport Canada is gratefully acknowledged. The authors wish to thank Mr. Roy Nishizaki, Senior Development Officer, TDC, for his valuable guidance during the course of this research; Mr. Jack Ritchie, Bender Machine Inc., for his suggestions on the use of stainless steel coatings; TAFA Inc. for supplying the coated specimens; and Metco Inc. for supplying the chrome oxide powder. Technical suggestions from Professors J.R. Cahoon and M.C. Chaturvedi throughout this research are also gratefully acknowledged.

References

1. H. Herman, "Coatings and Coating Practices," *Adv. Mater. Proc.*, *137*(1), Jan, 59-60, 84-85 (1990).
2. H. Herman, "Plasma-Sprayed Coatings," *Sci. Am.*, *259*(3), Sept, 112-117 (1988).
3. J. Ritchie, "Selecting Thermal Spray Coatings for the Repair of Equipment Parts by the Job Shop," *Proc. 2nd Nat. Conf. Thermal Spray*, Long Beach, Oct 31-Nov 2, ASM International, 87-90 (1984).
4. M.L. Thorpe, "Recent Advances in Arc Coating Technology and Equipment," *Proc. 2nd Nat. Conf. Thermal Spray*, Long Beach, Oct 31-Nov 2, ASM International, 91-100 (1984).
5. A.R. Jones, "Microcracks in Hard Chromium Electrodeposits," *Plat. Surf. Finish.*, April, 62-66 (1989).
6. D.T. Gawne and U. Ma, "Friction and Wear of Chromium and Nickel Coatings," *Wear*, *129*(1), 123-142 (1989).
7. M.G. El-Sherbiny, "Cylinder Liner Wear," *Proc. 9th Leeds-Lyon Symp. Triboloy*, Leeds, England, Sept 7-10, 182 (1982).

8. Y. Suzuki, S. Tanoue, and H. Yamaguchi, "Ceramic Coating on Engine Parts," *Proc. Conf. Surface Modifications and Coatings*, Toronto, Oct 14-16, ASM International 45-48 (1985).
9. Y. Suzuki, "Surface Modifications of Pistons and Cylinder Liners," *Proc. Conf. Surface Modifications and Coatings*, Toronto, Oct 14-16, ASM International, 49-57 (1985).
10. A.K. Murthy, K. Komvopoulos, and S.D. Brown, "Processing and Characterization of Multi-Layered Wear-Resistant Ceramic Coatings," *Trans. ASME, J. Eng. Mater. Technol., 112*, April, 164-174 (1990).
11. K.F. Dufrane and W.A. Glasser, "Wear of Ceramics in Advanced Heat Engine Applications," *Proc. Int. Conf. Wear of Materials*, Houston, April 5-9, 285-291 (1987).
12. V. Aronov and T. Mesyef, "Wear in Ceramic/Ceramic and Ceramic/Metal Reciprocating Sliding Contact," Part 1, *Trans. ASME, J. Tribology, 108*, Jan, 16-21 (1986).
13. T.E. Fischer, "Friction and Wear of Ceramics," *Scr. Metall. Mater., 24*, 833 (1990).
14. A.R. Rosenfield, "Wear and Fracture Mechanics: Are they Related?," *Scr. Metall. Mater., 24*, 811 (1990).
15. M.F. Ashby and S.C. Lim, "Wear-Mechanism Maps," *Scr. Metall. Mater., 24*, 805-810 (1990).
16. H.G. Wang and H. Herman, "Structure and Properties of Plasma Sprayed Spinel," *Ceram. Bull., 68*,(1), 97-102 (1989).
17. G.C. Barber and K.C. Ludema, "The Break-in Stage of Cylinder-Ring Wear: A Correlation Between Fired Engines and a Laboratory Simulator," *Wear, 118*, 57-75 (1987).
18. T. Akagaki and K. Kato, "Wear Mode Diagram in Lubricated Sliding Friction of Carbon Steel," *Wear, 129*, 303-317 (1989).
19. O.O. Ajayi and K.C. Ludema, "Mechanism of Transfer Film Formation During Repeat Pass Sliding of Ceramic Materials," *Wear, 140*,(2), Nov, 191 (1990).
20. S. Fein, Richard, "Boundary Lubrication," *Handbook of Lubrication*, CRC Press, Boca Raton, Florida, USA, 49-68 (1983).